



HAL
open science

Decrease in $\alpha\beta/\gamma\delta$ T-cell ratio is accompanied by a reduction in high-fat diet-induced weight gain, insulin resistance, and inflammation

Gwenaëlle Le Menn, Brigitte Sibille, Joseph Murdaca, Anne-Sophie Rousseau, Raphaëlle Squillace, Bastien Vergoni, Mireille Cormont, Isabelle Niot, Paul Grimaldi, Isabelle Mothe-Satney, et al.

► To cite this version:

Gwenaëlle Le Menn, Brigitte Sibille, Joseph Murdaca, Anne-Sophie Rousseau, Raphaëlle Squillace, et al.. Decrease in $\alpha\beta/\gamma\delta$ T-cell ratio is accompanied by a reduction in high-fat diet-induced weight gain, insulin resistance, and inflammation: $\alpha\beta/\gamma\delta$ T cell ratio effects on obesity. *FASEB Journal*, 2019, 33 (2), pp.2553-2562. 10.1096/fj.201800696RR . inserm-02473299

HAL Id: inserm-02473299

<https://inserm.hal.science/inserm-02473299>

Submitted on 10 Feb 2020

HAL is a multi-disciplinary open access archive for the deposit and dissemination of scientific research documents, whether they are published or not. The documents may come from teaching and research institutions in France or abroad, or from public or private research centers.

L'archive ouverte pluridisciplinaire **HAL**, est destinée au dépôt et à la diffusion de documents scientifiques de niveau recherche, publiés ou non, émanant des établissements d'enseignement et de recherche français ou étrangers, des laboratoires publics ou privés.

Decrease in $\alpha\beta/\gamma\delta$ T cell ratio is accompanied by a reduction in high fat diet-induced weight gain, insulin resistance, and inflammation

Short running title: $\alpha\beta/\gamma\delta$ T cell ratio effects on obesity

Gwenaëlle Le Menn¹, Brigitte Sibille¹, Joseph Murdaca¹, Anne-Sophie Rousseau¹, Raphaëlle Squillace¹, Bastien Vergoni¹, Mireille Cormont¹, Isabelle Niot², Paul A. Grimaldi^{1,†}, Isabelle Mothe-Satney¹, and Jaap G. Neels^{1,Δ}

¹ Université Côte d'Azur, Inserm, C3M, Nice, France

² Physiologie de la Nutrition et Toxicologie (NUTox), UMR U866 INSERM/Université de Bourgogne/AgroSup
Dijon, F-21000, Dijon, France.

^ΔCorresponding author

[†]Deceased May 16th, 2016

Address correspondence to:

Jaap G. NEELS

INSERM U 1065, Mediterranean Centre for Molecular Medicine (C3M)

Team 9: Metabolic challenges of immune cells in obesity, diabetes, and cardiovascular disease

Université de Nice-Sophia Antipolis

Bâtiment Universitaire Archimède (room M3-109bis)

151 Route de Ginestière BP 2 3194

06204 Nice Cedex 3

FRANCE

Phone: ++ 33 (0) 4 89 06 42 66

Fax: ++ 33 (0) 4 89 06 42 21

Email : Jaap.Neels@unice.fr

1 **Abbreviations:**

2	Acaa1	3-ketoacyl-CoA thiolase
3	ACC1	Acetyl-CoA carboxylase 1
4	ApoB	Apolipoprotein B
5	ATGL	Adipose triglyceride lipase
6	BAT	Brown adipose tissue
7	β 3AR	β -3 adrenergic receptor
8	Cpt1a	Carnitine O-palmitoyltransferase 1a
9	DGAT1	Diacylglycerol O-acyltransferase 1
10	EPI-WAT	Epididymal white adipose tissue
11	FAS	Fatty acid synthase
12	FFA	Free fatty acids
13	G6PDH	Glucose-6-phosphate 1-dehydrogenase
14	GPAT1	Glycerol-3-phosphate acyltransferase 1
15	GTT	Glucose tolerance test
16	HFD	High fat diet
17	HSL	Hormone-sensitive lipase
18	IR	Insulin resistance
19	LXR α	liver X receptor α
20	MCP-1	Monocyte chemoattractant protein 1
21	MTTP	Microsomal triglyceride transfer protein
22	NC	Normal chow
23	PAI-1	Plasminogen activator inhibitor 1
24	PGC1 α	Peroxisome proliferator-activated receptor gamma coactivator 1 α
25	PPAR β	Peroxisome Proliferator-Activated Receptor β
26	RER	Respiratory exchange ratio
27	SCD1	Acyl-CoA desaturase 1
28	SC-WAT	Subcutaneous white adipose tissue
29	SREBP1c	Sterol regulatory element-binding protein 1
30	SVF	Stromal vascular fraction
31	TCR	T cell receptor
32	Tg	Transgenic
33	TG	Triglycerides

- 1 Th T helper
- 2 Treg Regulatory T cell
- 3 UCP-1 Uncoupling protein 1
- 4 VLCAD Very long-chain specific acyl-CoA dehydrogenase
- 5 WAT White adipose tissue

6
7

1 **Abstract**

2

3 The implication of $\alpha\beta$ - and $\gamma\delta$ -T cells in obesity-associated inflammation and insulin resistance (IR) remains
4 uncertain. Mice lacking $\gamma\delta$ -T cells show either no difference or a decrease in high fat diet (HFD)-induced IR,
5 whereas partial depletion in $\gamma\delta$ -T cells does not protect from HFD-induced IR. $\alpha\beta$ -T cell deficiency leads to a
6 decrease in white adipose tissue (WAT) inflammation and IR without weight change, but partial depletion of
7 these cells has not been studied. We previously described a mouse model overexpressing Peroxisome
8 Proliferator-Activated Receptor β (PPAR β) specifically in T cells (Tg T-PPAR β) that exhibits a partial
9 depletion in $\alpha\beta$ -T cells and no change in $\gamma\delta$ -T cell number. This results in a decreased $\alpha\beta/\gamma\delta$ -T cell ratio in
10 lymphoid organs. We now show that Tg T-PPAR β mice are partially protected against HFD-induced weight
11 gain and exhibit decreased IR and liver steatosis independently of animal weight. These mice display an
12 alteration of WAT-depots distribution with an increased Epididymal-WAT mass and a decreased Subcutaneous-
13 WAT mass. Immune cell number is decreased in both WAT-depots, except for $\gamma\delta$ -T cells that are increased in
14 Epididymal-WAT. Overall, we show that decreasing $\alpha\beta/\gamma\delta$ -T cell ratio in WAT-depots alters their inflammatory
15 state and mass repartition which might be involved in improvement of insulin sensitivity.

16

17

18 **Keywords:** Obesity, adipose tissue, immune cells

19

1 INTRODUCTION

2 Obesity is associated with chronic white adipose tissue (WAT) and systemic inflammation leading to insulin
3 resistance (IR), type 2 diabetes, and cardiovascular diseases (1). Adipose tissue inflammation results from a
4 shift in the balance of anti-inflammatory towards pro-inflammatory immune cells. This shift is accompanied by
5 an elevation of pro-inflammatory cytokine secretion, such as IL-6 and TNF- α , that contribute to a disruption of
6 the insulin signaling pathways leading to IR (1). While macrophages are quantitatively the most abundant
7 immune cells in obese WAT, and their regulatory role in obesity-associated inflammation and IR has been
8 studied most extensively, T cells also play a critical regulatory role (1). Indeed, T cells infiltrate WAT before
9 macrophages, triggering the recruitment of the latter in the tissue (2).

10 T cells can be separated roughly into two populations based on the expression of different T cell receptor
11 heterodimers (TCR $\alpha\beta$ + or TCR $\gamma\delta$ +) and are referred to as $\alpha\beta$ and $\gamma\delta$ T cells, respectively. CD8+ cytotoxic T
12 cells and the different subsets of helper T cells (Th1, Th2, Th17, and Treg) generally belong to the $\alpha\beta$ T cells,
13 while $\gamma\delta$ T cells display broad functional plasticity and can behave differently depending on local presence of
14 cytokines and/or interaction with neighboring cells (3).

15 Both $\alpha\beta$ and $\gamma\delta$ T cells were shown to accumulate in obese WAT (4, 5). However, the specific contribution of
16 $\alpha\beta$ and $\gamma\delta$ T cells to obesity-associated inflammation and IR remains uncertain. Indeed, one study detected no
17 difference in HFD-induced IR between mice lacking $\gamma\delta$ T cells (TCR $\delta^{-/-}$ mice) and wild-type control mice (6),
18 whereas another study showed that these same HFD-fed mice had less inflammation and IR (7). In contrast,
19 mice lacking 70% of $\gamma\delta$ T cells in WAT (V γ 4/6 $^{-/-}$ mice) were not protected from HFD-induced IR, but WAT
20 inflammation was still reduced (7). Regarding the role of $\alpha\beta$ T cells, mice completely devoid of $\alpha\beta$ T cells were
21 studied (TCR $\beta^{-/-}$ mice), which exhibit suppressed macrophage infiltration and reduced inflammatory cytokine
22 expression in WAT, and are partially protected against HFD-induced IR compared to wild-type obese controls
23 (8). It has not been studied whether, similar to $\gamma\delta$ T cells, a partial lack compared to a complete absence of $\alpha\beta$ T
24 cells leads to different phenotypes.

25 We have previously developed a transgenic mouse model that overexpresses the transcription factor Peroxisome
26 Proliferator-Activated Receptor β (PPAR β) specifically in T cells (9). This PPAR β overexpression inhibits $\alpha\beta$ T
27 cell development in the thymus and as a result these Tg T-PPAR β mice exhibit a \pm 70% reduction in $\alpha\beta$ T cells.
28 The remaining 30% of $\alpha\beta$ T cells that manage to develop do not overexpress PPAR β (9). We used this
29 transgenic mouse model as a tool to investigate the effect of a partial lack of $\alpha\beta$ T cells on HFD-induced obesity
30 and its associated inflammation and IR. More specifically, we studied the effects of HFD feeding on weight,
31 food intake/lipid absorption, liver steatosis, WAT immune cell infiltration, plasma and WAT cytokine levels,
32 and glucose- and insulin-tolerance of Tg T-PPAR β compared to control mice.

MATERIALS AND METHODS

Mouse studies

Animals were maintained in a 12-h light, 12-h dark cycle and received food and water ad libitum. All experimental procedures were conducted according to French legislation and approved by the Ministère de l'Enseignement supérieur, de la Recherche et de l'Innovation and the Animal Care Committee of the Faculty of Medicine of the Nice Sophia Antipolis University (Comité Institutionnel d'Éthique Pour l'Animal de Laboratoire)(APAFIS#3617-201601 0615481008). Both strains used in this study are on the C57BL/6J background. Lck-Cre mice, used as control, were obtained from Jackson laboratory (B6.Cg-Tg(Lck-cre)548Jxm/J, stock number 003802). Double transgenic animals that overexpress PPAR β specifically in T cells (Lck-Cre/CAG-Stop-PPAR β mice), and previously described (9), are referred as Tg T-PPAR β mice. 12 weeks old male mice were fed with a normal chow (NC, 8.4% kcal from fat; A04; Safe Diets) or a high fat diet (HFD, 60% kcal from fat; 58Y1; TestDiets) for 17 weeks. Body weight and food intake were measured every week, whereas insulin and glucose tolerance tests were respectively performed at 11 and 13 weeks of the diet. Food intake was measured as Kcal/week normalized by mice weight and food efficiency ratio was measured as 100x(mean weight gain (g)/mean food intake (g)).

Glucose and insulin tolerance test

After 5h of fasting, mice were injected ip with glucose (1g/kg) for glucose tolerance test (GTT) or insulin (0.65U/kg) for insulin tolerance test (ITT). Plasma glucose was measured 0, 15, 30, 60 and 120 min after injection with the One-Touch Verio Pro+ glucose-monitoring system (Lifescan). Insulinemia was quantified 0, 15 and 30 min after glucose injection during GTT with an ultra-sensitive rat insulin Elisa kit (Crystal Chem). HOMA-IR (Homeostatic Model Assessment for Insulin Resistance) index was calculated based on fasting plasma insulin and glucose values at T0 of the GTT using the formula insulin [mU/L] x glucose [mMol/L]/14.1, then values were normalized to 1 for control mice on NC.

Indirect calorimetry cages

Indirect calorimetry was performed at 13 weeks of diet. Twenty-four hours prior to data collection, mice were placed in separate calorimetry chambers with free access to food and water. Temperature was maintained at 22°C and the light was on from 07:00 to 19:00 hours. O₂ consumption (VO₂) and CO₂ production (VCO₂) were measured (Oxylet; Panlab-Bioseb, Vitrolles, France) in individual mice at 25 min intervals during a 24-h period. The respiratory exchange ratio ([RER] = VCO₂/VO₂) and Energy expenditure (in kcal/day/kg^{0.75}) were calculated.

1 Ambulatory activities of the mice were monitored using a weight sensor coupled to an infrared photocell beam
2 interruption method (Panlab-Bioseb).

4 **Flow cytometry**

5 For WAT vascular stromal fraction analysis, epididymal and sub-cutaneous adipose tissue (0.5-1 g) were
6 harvested from control and Tg-T-PPAR β mice. Tissues were rinsed with PBS and cut into small pieces in PBS
7 supplemented with 0.5% bovine serum albumin (BSA) before digestion (20 minutes, 37°C, 160 rpm) with
8 collagenase clostridium histolyticum (1mg/ml, Sigma). After filtration (100 μ m) and centrifugation (5 minutes
9 at 300g), stromal vascular fraction was pelleted.

10 The resulting single cell suspensions were incubated with Fc Block (anti-mouse CD16/CD32 monoclonal
11 antibody, BD Biosciences) for 15 min at 4°C before staining with fluorescently labeled primary antibodies for
12 20 min at 4°C in PBS, 0.5% BSA. α CD3-fluorescein isothiocyanate, α CD4-allophycocyanin, α TCR β -
13 phycoerythrin-Cy7, α TCR $\gamma\delta$ -phycoerythrin, α F4/80- allophycocyanin, α CD11b-phycoerythrin-Cy7, and
14 α CD11c-phycoerythrin were purchased from eBioscience. CD8-Peridinin chlorophyll antibody was from BD
15 Biosciences. Cells were gently washed twice and resuspended in PBS, 0.5% BSA with DAPI. Stained cell
16 preparations were analyzed using a BD FACSCanto II flow cytometer (BD Biosciences).

18 **RNA extraction and quantitative real time PCR**

19 Total RNA were extracted from tissues with Trizol reagent following the supplier's protocol (Invitrogen). Total
20 RNA (1 μ g) were reverse-transcribed using a QuantiTect Reverse Transcription Kit (Qiagen). Quantitative PCR
21 was done using SYBR Premix Ex Taq (Tli RNase H Plus) (Ozyme) on a StepOne machine (Life Technologies).
22 The mRNA levels of all genes reported were normalized to 36B4 transcript levels. Data was analyzed using the
23 $\Delta\Delta$ Ct method. Primer sequences are available upon request.

25 **Blood analysis**

26 After the 17 weeks of diet, blood was collected from non-fasted mice by intra-cardiac puncture using a 22Gx1½
27 needle and S-monovette syringe coated with EDTA and then centrifuged to obtained plasma samples. Total
28 cholesterol (ref: STA-390, Cell biolabs), and endotoxin (ref: 88282, Thermo scientific) were measured in
29 plasma according to the protocols provided by the manufacturer. Free fatty acid (ref: K612-100, Biovision)
30 were measured in the plasma of 4h fasted mice collected during GTT following the manufacturer's protocol.

1 **FITC-dextran assay**

2 *In vivo* intestinal permeability assay in small intestine and colon was performed using an FITC- dextran assay.
3 After 5h of fasting, mice were received an oral gavage with 150µL of FITC-dextran 4KDa (80mg/ml). Blood
4 was collected from the caudal vein 1 and 4h after oral gavage and fluorescence intensity was measured in the
5 plasma (Excitation: 485 nm, Emission: 528 nm) to assess small intestine and colon permeability, respectively.
6

7 **Lipid quantification in feces**

8 Stool lipids were extracted from an aliquot of feces (200 mg) collected during 24 h using the Folch method
9 (10).
10

11 **Protein quantification in epididymal adipose tissue**

12 Epididymal adipose tissue (250 mg approximatively) was homogenized in PBS using tubes containing ceramic
13 beads and run in a tissue grinder (Precellys) for 5 sec at 6500 rpm. Samples were then centrifuged for 1 min at
14 4°C and 2500 rpm. The intermediary phase containing proteins was removed and submitted to thermal shock
15 twice (freezing in liquid nitrogen followed by thawing at 37°C). Samples were centrifuged for 5 min at 4°C and
16 5000 g and total protein concentration was determined using Bradford assay (Biorad). IL-17a ELISA (ref:
17 860.070.096, Diaclone) and Luminex technology (ref: MADKMAG-71K, Merck) were used to measure IL-17,
18 IL-6, MCP-1, TNF-α, PAI-1, resistin and leptin in epididymal adipose tissue lysates. All quantifications were
19 done according to the protocols provided by the manufacturer.
20

21 **Liver triacylglycerol**

22 Liver triacylglycerol concentration was estimated from glycerol release after ethanolic KOH hydrolysis, using a
23 commercial colorimetric kit (ref: F6428, Sigma).
24

25 **Histology**

26 Epididymal and sub-cutaneous adipose tissue and liver were fixed in 10% formalin before embedding in
27 paraffin. Seven-micrometer tissue sections were deparaffinized, rehydrated and stained with hematoxylin (5
28 min) and eosin (30sec-1min). The Zeiss Microdissector PALM was used to analyze liver and adipose tissue
29 slides. Adipocyte area was determined by the software Adiposoft.
30

1 **Statistics**

2 All calculations were performed using Prism 5.0 software (GraphPad, San Diego, CA). Statistical significance
3 between groups was determined by two-way ANOVA, Mann-Whitney or Kruskal-Wallis tests. Differences
4 were considered statistically significant when $p < 0.05$.

5

1 RESULTS

2 Tg T-PPAR β mice are partially protected against diet-induced obesity

3 Tg T-PPAR β mice, that overexpress PPAR β specifically in T cells, were generated by our laboratory as
4 described previously (9). These mice were shown to have an impaired $\alpha\beta$ T cell development leading to a
5 decrease in $\alpha\beta$ T cells but no change in $\gamma\delta$ T cell number (decrease in $\alpha\beta/\gamma\delta$ T cell ratio). We decided to
6 investigate the consequences of this change in T cell population on obesity-associated inflammation and insulin
7 resistance. Control and Tg T-PPAR β mice were fed with a normal chow or a high-fat diet for 17 weeks during
8 which body weight and food intake were measured every week. On NC, Tg T-PPAR β mice had the tendency to
9 have a lower weight throughout the 17-week period compared to control mice but this difference was not
10 significant (**Fig. S1A**). However, Tg T-PPAR β mice fed a HFD, show a 10% decrease in final weight compared
11 with control mice after 17 weeks of diet, with a significant difference observed as early as 2 weeks after starting
12 the diet (**Fig. 1A** and **S1A**). Mean quantification of food intake (**Fig. 1B**) and food efficiency ratio (**Fig. 1C**)
13 show no difference between HFD-fed Tg T-PPAR β and control mice.

14 NC- and HFD-fed groups were then placed in indirect calorimetry cages to measure their activity and energy
15 expenditure. HFD-fed Tg T-PPAR β mice exhibited an increase in rearing activity, compared to their control
16 counterpart (**Fig. 1D**), without modification of their energy expenditure (**Fig. 1E**) and RER (data not shown).
17 No differences in activity and energy expenditure were observed in mice on NC (**Fig. S1B** and **S1C**). However,
18 adipose tissue (BAT) capacity to convert energy into heat seems to be increased in HFD-fed Tg T-PPAR β mice,
19 as reflected by an upregulation of mRNA encoding the thermogenic uncoupling protein 1 (UCP1) as well as
20 CIDEA another molecular marker of brown adipocytes, while two others genes were unchanged (peroxisome
21 proliferator-activated receptor gamma coactivator 1 alpha (PGC1 α) and β -3 adrenergic receptor (β 3AR)) (**Fig.**
22 **1F**).

23
24 Next, we measured intestinal permeability as it is known to increase in obesity and could alter mice body
25 weight (11). For this we used three different measures: 1) Total lipid in feces (as an indicator of intestinal lipid
26 absorption), 2) FITC-dextran appearance in blood (after oral gavage), and 3) plasma endotoxin levels. None of
27 those measures revealed any differences (**Figs. 1G, S1D, and S1E**), suggesting that intestinal permeability is
28 similar between HFD-fed Tg T-PPAR β and control mice. Plasma lipids such as free fatty acids and cholesterol
29 were also quantified in NC and HFD-fed mice and no difference was found between the different genotypes on
30 the same diet. However, we observed an effect of the HFD with an increase in cholesterol and decrease in FFA
31 concentrations compared with NC-fed mice (**Table 1**).

1 **Obese Tg T-PPAR β mice exhibit an amelioration of glucose homeostasis and insulin sensitivity**
2 **independent of a difference in weight gain.**

3 Next, we investigated glucose homeostasis and insulin sensitivity. We performed insulin and glucose tolerance
4 tests (ITT/GTT) on our 4 groups of mice at week 11 and 13 of the diet, respectively, and measured plasma
5 insulin concentration in response to glucose injection during GTT. In our study, HFD groups exhibit a
6 significant difference in weight gain between genotypes. As weight gain is known to be positively correlated
7 with glucose intolerance and insulin resistance in diet-induced obesity (12), we decided to use weight-matched
8 HFD-fed Tg T-PPAR β and control mice for the following analysis. In the NC groups, no significant difference
9 in blood glucose concentration during the GTT or ITT, plasma insulin level, and the homa-IR index was
10 observed between control and Tg T-PPAR β mice as shown in **Fig. 2**. As expected, when challenged with an
11 HFD, control mice develop signs of glucose intolerance and insulin resistance demonstrated by elevated blood
12 glucose concentrations during GTT and ITT, and increased insulin secretion compared with control mice under
13 a normal diet (**Fig. 2A-C**). HFD-fed Tg T-PPAR β mice have a significantly decreased blood glucose
14 concentration during GTT and ITT accompanied by a 2-fold decrease in GTT-associated plasma insulin level
15 compared with HFD-fed control mice (**Fig. 2A-C**). Homa-IR index, reflecting mice insulin sensitivity, is
16 subsequently decreased by 47% in Tg T-PPAR β HFD-fed mice (1.88 AU) compared with their weight-matched
17 control (3.99 AU), but stay higher than NC-fed control (1 AU) (**Fig. 2D**). HFD-fed Tg T-PPAR β mice have an
18 intermediate phenotype where they develop a HFD-induced partial glucose intolerance and insulin resistance.
19 Taken together, our results suggest that T cell population changes found in Tg T-PPAR β mice don't seem to
20 have consequences for weight gain, glucose homeostasis and insulin resistance when mice are fed with a normal
21 diet. However, on a high-fat diet these mice exhibit a reduction in weight gain and ameliorated metabolic
22 parameters, the latter being independent of the weight gain reduction.

23
24 **HFD-induced liver steatosis is decreased in Tg T-PPAR β mice compared to control mice**

25 Since differences in body weight and glucose homeostasis were only evident between HFD-fed groups, we
26 decided to focus only on the latter groups for the remainder of the study. With an improvement in whole-body
27 insulin sensitivity in HFD-fed Tg T-PPAR β mice, we wanted to investigate other insulin-sensitive organs like
28 the liver. Liver weight significantly decreases from an average of 2000 \pm 109 mg in control mice to an average
29 of 1500 \pm 89 mg in Tg T-PPAR β mice at the end of the diet (**Fig. 3A**). After normalizing to mice body weight,
30 the difference could still be observed, suggesting that liver weight decrease in HFD-fed Tg T-PPAR β mice is
31 not only the result of their decreased weight gain (**Fig. S2**). Triglycerides (TG) are known to increase in the
32 liver during obesity leading to hepatic steatosis, so liver triglycerides were measured in our HFD-fed groups. A
33 50% decrease of liver TG levels in Tg T-PPAR β mice was observed (**Fig. 3B**) and confirmed by histology with

1 a hematoxylin/eosin staining showing less lipid droplet accumulation (in white) in the Tg T-PPAR β mice (**Fig.**
2 **3C**). Liver lipid content is regulated by lipid transport (import and export), oxidation, and lipogenesis. We
3 decided to analyze the mRNA level of genes implicated in these different pathways. First, we quantified relative
4 mRNA levels of genes implicated in lipid transport such as fatty acid translocase (Fat/CD36), apolipoprotein B
5 (ApoB), and microsomal triglyceride transfer protein (MTTP). mRNA levels of Fat/CD36 regulating lipid
6 import into the liver was downregulated by half of the control, while ApoB and MTTP implicated in lipid
7 export into the blood were unchanged in Tg T-PPAR β mice (**Fig. 3D**). These results suggest that lipid transport
8 is altered in livers of Tg T-PPAR β mice with a lower entry of lipids in the liver but no modification in the lipid
9 export out of the liver. Next, genes implicated in lipid metabolism, either lipolysis/ β oxidation or
10 lipogenesis/esterification, were examined. mRNA levels of adipose triglyceride lipase (ATGL) and hormone-
11 sensitive lipase (HSL) (first two-step enzymes of TG lipolysis) were downregulated in liver of Tg T-PPAR β
12 mice. mRNA levels of PPAR α (driver of hepatic lipid oxidation) as well as its coactivators (PGC1- α and - β),
13 and its target genes carnitine O-palmitoyltransferase 1a (Cpt1a), very long-chain specific acyl-CoA
14 dehydrogenase (VLCAD), and 3-ketoacyl-CoA thiolase (Acaa1) were then analyzed. Both PGC1- α and - β were
15 shown to be downregulated in liver of Tg T-PPAR β mice whereas mRNA levels of PPAR α , Cpt1a, VLCAD,
16 and Acaa1 were similar compared to the control group (**Fig. 3E**). mRNA levels of lipogenic genes (liver X
17 receptor alpha (LXR α), fatty acid synthase (FAS), diacylglycerol O-acyltransferase 2 (DGAT2), glucose-6-
18 phosphate 1-dehydrogenase (G6PDH), and acyl-CoA desaturase 1 (SCD1)) were decreased in our Tg T-PPAR β
19 mice whereas acetyl-CoA carboxylase 1 (ACC1), diacylglycerol O-acyltransferase 1 (DGAT1), and sterol
20 regulatory element-binding protein 1 (SREBP1c) mRNA levels were unchanged (**Fig. 3F**). Lipid oxidation
21 didn't seem to be affected in Tg T-PPAR β mice while lipolysis and de novo lipogenesis/esterification seem to
22 be inhibited. We then decided to measure relative mRNA levels of inflammatory markers. mRNA levels of
23 CD68 and CD3 respectively used as macrophage and T cell markers were downregulated in livers of Tg T-
24 PPAR β mice compare with control mice (**Fig. 3G**). Liver cytokine mRNA levels such as interleukin 6 (IL-6),
25 IL-1 β , tumor necrosis factor alpha (TNF- α), and transforming growth factor-beta (TGF β) were similar between
26 Tg T-PPAR β and control mice whereas monocyte chemotactic protein 1 (MCP-1) expression was decreased in
27 Tg T-PPAR β mice (**Fig. 3G**). These results suggest a decrease of macrophages and lymphocytes infiltration in
28 the liver of Tg T-PPAR β mice.

29 Overall, Tg T-PPAR β mice have less hepatic steatosis that may be due to a reduction in lipid import and hepatic
30 de novo lipogenesis/esterification, and show a decrease in liver macrophage and T cell markers.

1 **Adipose tissue distribution and function are altered in Tg T-PPAR β mice**

2 White adipose tissue (WAT) is a key organ in the development of obesity associated insulin resistance. As Tg
3 T-PPAR β mice exhibit ameliorated insulin sensitivity with less hepatic steatosis we decided to look at adipose
4 tissue function. Among the different adipose tissue depots, we analyzed the epididymal (EPI-WAT) and
5 subcutaneous inguinal (SC-WAT) adipose depots that are most commonly studied. Both tissues were weighed
6 after 17 weeks of HFD, and histology (hematoxylin/eosin staining) was performed to measure mean adipocyte
7 area. Adipose tissue repartition was altered in our HFD-fed Tg T-PPAR β mice with an increase in EPI-WAT
8 and a decrease in SC-WAT compared with HFD-fed control mice (**Fig. 4A**). As shown in **Fig. 4B**, mean
9 adipocyte area was higher in SC-WAT of Tg T-PPAR β mice, whereas no change was observed in the EPI-WAT
10 compared to their control counterpart. We next investigated the metabolic activity of these two different adipose
11 tissue depots by measuring adipose mRNA levels of genes implicated in lipid metabolism with either lipogenic
12 genes (ACC1, FAS, DGAT1, DGAT2, lipin1, glycerol-3-phosphate acyltransferase 1 (GPAT1)) or lipolytic
13 genes (ATGL, HSL). Even though FAS and DGAT2 mRNA levels tend to be downregulated, none of the eight
14 genes analyzed were significantly modified in the SC-WAT between Tg T-PPAR β and control mice (**Fig. 4C**).
15 In EPI-WAT of Tg T-PPAR β mice, lipolytic genes such as ATGL and HSL exhibit a 1.5-fold induction
16 compared with control mice with an upregulation of lipogenic genes (between 1.2 and 1.7-fold) except for
17 ACC1 mRNA level which is not significantly changed (**Fig. 4D**).

18 These results suggest that HFD-fed Tg T-PPAR β mice exhibit a change in WAT distribution and a concomitant
19 increase in mRNA levels of members of lipogenesis/esterification and lipolysis pathways only in EPI-WAT.

21 **Decreased adipose tissue inflammation and $\alpha\beta/\gamma\delta$ T cell ratio in HFD-fed Tg T-PPAR β mice**

22 Next, we decided to investigate the immune cell composition in the WAT of our HFD-induced obese mice. SVF
23 was isolated from the EPI-WAT and SC-WAT of Tg T-PPAR β and control mice and immune cells analyzed by
24 flow cytometry.

25 In Tg T-PPAR β mice, the total number of cells found in the SVF was decreased compared to control mice in
26 either EPI-WAT and SC-WAT (data not shown). Total macrophages were distinguished by using the F4/80
27 marker. Then, pro-inflammatory (F4/80+ CD11b+ CD11c+) and anti-inflammatory (F4/80+ CD11b+ CD11c-)
28 macrophages were quantified. Similar observations concerning macrophage populations were obtained in Tg T-
29 PPAR β SC-WAT (**Fig. S3**) and EPI-WAT (**Fig. 5**).

30 In EPI-WAT, the percentage of total macrophages ($\approx 20\%$) was similar between both genotypes, but a shift from
31 CD11c+ toward CD11c- macrophages was observed in the Tg T-PPAR β mice (**Fig. 5A**). Quantification of
32 macrophage subpopulations (**Fig. 5B**) showed a decrease in total and CD11c+ macrophage number whereas the
33 CD11c- macrophage number was unchanged in Tg T-PPAR β mice, leading to a decrease of CD11c+/CD11c-

1 ratio (**Fig. 5C**). Then, T cell subpopulations were identified in the EPI-WAT SVF based on the expression of
2 CD3, TCR β , TCR $\gamma\delta$, CD4 and CD8 markers. Percentage of total T lymphocytes (CD3+), as well as cell
3 number, was not significantly different between Tg T-PPAR β and control mice, whereas $\alpha\beta$ and $\gamma\delta$ T cell
4 population repartition was altered. $\gamma\delta$ T cell proportion was increased in EPI-WAT of Tg T-PPAR β mice (50%
5 vs 30% in control mice) while $\alpha\beta$ T cell proportion was decreased in Tg T-PPAR β mice (**Fig. 5D**). While CD4
6 and CD8 T cell percentages were slightly decreased, these differences were not statistically significant.
7 Quantification of T cell number showed an increase in $\gamma\delta$ T cells associated with a tendency to $\alpha\beta$ T cell number
8 reduction ($p < 0.051$) in Tg T-PPAR β mice (**Fig. 5E**), leading to a decrease in $\alpha\beta/\gamma\delta$ T cell ratio (**Fig. 5F**). In the
9 SC-WAT of Tg T-PPAR β mice, $\gamma\delta$ T cell proportion was increased (35% vs 10% in control group) without
10 increasing $\gamma\delta$ T cell number (**Fig. S3D-E**). However, $\alpha\beta$ and CD4 T cell number were significantly decrease in
11 Tg T-PPAR β mice (**Fig. S3E**). Similar to EPI-WAT, the $\alpha\beta/\gamma\delta$ T cell ratio was decreased in SC-WAT from
12 HFD-fed Tg T-PPAR β mice (**Fig. S3F**). Concentration of inflammatory cytokines present in the EPI-WAT
13 were also measured (**Table 2**). Among the cytokines measured, IL-6, plasminogen activator inhibitor-1 (PAI-1),
14 and IL-17 were significantly decreased in EPI-WAT of Tg T-PPAR β mice compared with control mice while
15 MCP-1, resistin, and leptin concentrations were unchanged. TNF α levels were below the detection limit (data
16 not shown).
17 Overall, a decrease in $\alpha\beta/\gamma\delta$ T cell ratio in WAT was observed in Tg T-PPAR β mice with a concomitant
18 decrease in CD11c⁺ macrophages and pro-inflammatory cytokines.
19

1 DISCUSSION

2 In this study, we demonstrate that a decrease in $\alpha\beta/\gamma\delta$ T cell ratio has an impact on obesity-induced
3 inflammation and IR. These results are similar to some of the effects observed in the complete absence of $\alpha\beta$ T
4 cells (8). However, there is one major discrepancy; our mice lacking 70% of their $\alpha\beta$ T cells are partially
5 protected against HFD-induced weight gain, while mice that are completely deficient for $\alpha\beta$ T cells did not
6 exhibit a difference in HFD-induced weight gain compared to control mice (8). This differential effect on
7 weight gain due to partial versus complete absence of $\alpha\beta$ T cells presents an intriguing enigma. Indeed, we have
8 explored peripheral tissues and did not obtain results that could totally explain the reduced weight gain of our
9 Tg T-PPAR β mice. However, we did not investigate inflammation in the brain that has been shown to be
10 implicated in body weight regulation (13). We therefore can't rule out the possibility that we also have a
11 decrease in $\alpha\beta$ T cells in the brain and that this could affect mice body weight.

12 In addition, data from several studies suggest that T cell activation might be linked to weight gain. It was shown
13 that treatment of mice on an obesogenic diet with anti-CD40L antibody (blocks co-stimulation needed for T cell
14 activation), cyclosporine A (interferes with activity and growth of T cells), or fingolimod (inhibits T cell
15 emigration from lymphoid organs) leads to decreased weight gain (14, 15). This was accompanied by decreased
16 liver weight/steatosis, decreased (CD11c+) macrophage infiltration of WAT, and improved insulin sensitivity,
17 all phenotypes that we also observed in our Tg T-PPAR β mice. Another mouse model that shares many of the
18 phenotypes observed in our HFD-fed Tg T-PPAR β mice are mice deficient in major histocompatibility complex
19 class II (MHC-II^{-/-} mice) (16). Presentation of antigens by MHC-II molecules on antigen presenting cells to T
20 cells is crucial for the maturation of the latter. In addition to decreased weight gain, liver steatosis,
21 inflammation, and IR, MHC-II-deficient mice also exhibit an increase in EPI-WAT weight, similar to our Tg T-
22 PPAR β mice. Further research is merited to investigate the mechanisms behind this effect of T cell numbers and
23 activation status on weight gain.

24 With a higher lipolytic rate that favors lipid release in blood and at term lipotoxicity, EPI-WAT expansion is
25 commonly associated with insulin-resistance unlike the SC-WAT that has a better lipid storage capacity (17).
26 However, the increase in EPI-WAT weight observed in our HFD-fed Tg T-PPAR β mice (compared to control
27 mice) was not accompanied by increased metabolic dysfunction. Instead, the mice exhibited improved glucose
28 and insulin sensitivity. Many studies have indicated that WAT hypertrophy is strongly associated with the
29 development of insulin resistance while adipocyte hyperplasia is thought to ameliorate insulin sensitivity (18).
30 The increase in EPI-WAT in our Tg T-PPAR β mice was not accompanied by an increase in adipocyte
31 hypertrophy when compared to control mice, suggesting that this tissue instead expanded as a result of
32 adipocyte hyperplasia. This might explain why these mice exhibit improved glucose homeostasis, even though

1 EPI-WAT mass was increased. In this regard, it is of interest to mention that the increase in EPI-WAT observed
2 in MHC-II^{-/-} mice also appears to be due to adipocyte hyperplasia (16).

3 It was demonstrated that the AT microenvironment drives its growth and distribution in obesity, which suggests
4 that the local immune cell composition and secretion could have an impact on AT depot-specific adipogenesis
5 (19). We observed a decrease in $\alpha\beta/\gamma\delta$ T cell ratio in WAT, which was accompanied by a decrease in (CD11c+)
6 macrophages and the expression of certain pro-inflammatory cytokines. These differences could be implicated
7 in the observed alteration of repartition and metabolic function of the different WAT depots. For instance, IL-6,
8 PAI-1 and IL-17 levels are decreased in EPI-WAT from Tg T-PPAR β mice and all three factors have been
9 shown to inhibit adipogenesis (20-22). Therefore, the decrease in the levels of these adipogenesis inhibitors
10 might have led to the adipocyte hyperplasia that could explain the EPI-WAT expansion in our Tg T-PPAR β
11 mice.

12 In EPI-WAT from HFD-fed Tg T-PPAR β mice there is not only a proportional increase in $\gamma\delta$ T cells but also an
13 increase in their overall number. A similar increase in $\gamma\delta$ T cells was also observed in EPI-WAT from HFD-fed
14 TCR β ^{-/-} mice (8). This increase might be specific for EPI-WAT since we did not observe it in SC-WAT nor in
15 lymphoid tissues (9). The mechanism behind this EPI-WAT-specific increase in $\gamma\delta$ T cells that accompanies
16 (partial) $\alpha\beta$ T cell deficiency remains to be established.

17 One of the changes in metabolic function in EPI-WAT that we observed in our Tg T-PPAR β mice was the
18 simultaneous upregulation of genes implicated in the degradation and the formation of triglyceride lipid droplets
19 (lipolysis/lipogenesis pathways), which could constitute a futile cycle. Actually, we have studied the lipolysis/
20 lipogenesis pathway only by measuring mRNA levels coding for key enzymes. It would be interesting to
21 corroborate these results by measuring protein activity and/or measuring metabolic fluxes using radioactive
22 tracers.

23 A potential consequence of a futile cycle is an energy dissipation in the form of heat and here our data seems to
24 indicate the presence of a futile cycle in the EPI-WAT of Tg T-PPAR β that needs to be further explored.

25 Furthermore, our data suggest that the BAT tissue of Tg T-PPAR β mice has an increased thermogenesis
26 capacity compared to that of control mice. Finally, PPAR β mice seem to be more active compared with control
27 mice (on HFD). Taken together, these different observations suggest that Tg T-PPAR β mice might be
28 exhibiting a slight increase in energy expenditure that is not detectable in our metabolic cages but could explain
29 their decreased weight gain compared with control mice. However, further studies are needed to confirm a
30 potential increased thermogenesis in BAT of Tg T-PPAR β mice.

31
32 Collectively, our results demonstrate that a decrease in $\alpha\beta/\gamma\delta$ T cell ratio leads to a reduction in high fat diet-
33 induced weight gain. Furthermore, our Tg T-PPAR β mice are partially protected against obesity-induced IR

1 compared to control mice, independently of the reduced weight gain. This is accompanied by a decrease in liver
2 steatosis and inflammation, and changes in adipose tissue distribution, function, and immune cell content. These
3 results support the idea that targeting the $\alpha\beta/\gamma\delta$ T cell ratio could be a therapeutic approach for the treatment of
4 obesity and its associated inflammatory and metabolic dysfunctions.

5

1 **ACKNOWLEDGEMENTS**

2 The authors thank Véronique Corcelle and the INSERM U1065 animal facility staff for their excellent care of
3 mice. Image acquisition and image analysis were performed on the C3M Imaging Core Facility (part of
4 Microscopy and Imaging platform Côte d'Azur, MICA), with the help of Maeva Gesson. Furthermore, the
5 authors thank Giulia Chinetti and Philippe Gual (Université Côte d'Azur, CHU, Inserm, C3M, Nice, France) for
6 critical reading of the manuscript and scientific discussions, respectively.

7 **Author Contributions.** G.L.M., B.S., J.M., A.-S.R., R.S., B.V., I.N., P.A.G., I.M.-S., and J.G.N. performed the
8 experiments. G.L.M., B.S., I.N. I.M.-S., and J.G.N. analyzed the data. G.L.M., B.S., P.A.G., I.M.-S., and J.G.N.
9 conceived the study. G.L.M., B.S., I.M.-S., and J.G.N. wrote the manuscript. G.L.M., B.S., A.-S.R., M.C., I.N.,
10 I.M.-S., and J.G.N. reviewed/edited the manuscript. J.G.N. is the guarantor of this work and, as such, had full
11 access to all the data in the study and takes responsibility for the integrity of the data and the accuracy of the
12 data analysis.

13 **Duality of Interest.** No potential conflicts of interest relevant to this article were reported.

14 **Funding.** This work was financially supported by INSERM, the Université Côte d'Azur, the Fondation pour la
15 Recherche Médicale (FRM, Grant DRM20101220437), the French National Research Agency (ANR, N° ANR-
16 14-CE12-0008-02) and the Agence Française de Lutte contre le Dopage (AFLD).

17

18

1 REFERENCES

- 2
- 3 1. McLaughlin, T., Ackerman, S. E., Shen, L., and Engleman, E. (2017) Role of innate and adaptive immunity
- 4 in obesity-associated metabolic disease. *The Journal of clinical investigation* **127**, 5-13
- 5 2. Kintscher, U., Hartge, M., Hess, K., Foryst-Ludwig, A., Clemenz, M., Wabitsch, M., Fischer-Posovszky, P.,
- 6 Barth, T. F., Dragun, D., Skurk, T., Hauner, H., Bluher, M., Unger, T., Wolf, A. M., Knippschild, U.,
- 7 Hombach, V., and Marx, N. (2008) T-lymphocyte infiltration in visceral adipose tissue: a primary event in
- 8 adipose tissue inflammation and the development of obesity-mediated insulin resistance. *Arterioscler*
- 9 *Thromb Vasc Biol* **28**, 1304-1310
- 10 3. Paul, S., Singh, A. K., Shilpi, and Lal, G. (2014) Phenotypic and functional plasticity of gamma-delta
- 11 (gammadelta) T cells in inflammation and tolerance. *Int Rev Immunol* **33**, 537-558
- 12 4. Wu, H., Ghosh, S., Perrard, X. D., Feng, L., Garcia, G. E., Perrard, J. L., Sweeney, J. F., Peterson, L. E.,
- 13 Chan, L., Smith, C. W., and Ballantyne, C. M. (2007) T-cell accumulation and regulated on activation,
- 14 normal T cell expressed and secreted upregulation in adipose tissue in obesity. *Circulation* **115**, 1029-1038
- 15 5. Caspar-Bauguil, S., Cousin, B., Galinier, A., Segafredo, C., Nibbelink, M., Andre, M., Casteilla, L., and
- 16 Penicaud, L. (2005) Adipose tissues as an ancestral immune organ: site-specific change in obesity. *FEBS*
- 17 *letters* **579**, 3487-3492
- 18 6. Zuniga, L. A., Shen, W. J., Joyce-Shaikh, B., Pyatnova, E. A., Richards, A. G., Thom, C., Andrade, S. M.,
- 19 Cua, D. J., Kraemer, F. B., and Butcher, E. C. (2010) IL-17 regulates adipogenesis, glucose homeostasis,
- 20 and obesity. *Journal of immunology* **185**, 6947-6959
- 21 7. Mehta, P., Nuotio-Antar, A. M., and Smith, C. W. (2015) gammadelta T cells promote inflammation and
- 22 insulin resistance during high fat diet-induced obesity in mice. *Journal of leukocyte biology* **97**, 121-134
- 23 8. Khan, I. M., Dai Perrard, X. Y., Perrard, J. L., Mansoori, A., Smith, C. W., Wu, H., and Ballantyne, C. M.
- 24 (2014) Attenuated adipose tissue and skeletal muscle inflammation in obese mice with combined CD4+ and
- 25 CD8+ T cell deficiency. *Atherosclerosis* **233**, 419-428
- 26 9. Mothe-Satney, I., Murdaca, J., Sibille, B., Rousseau, A. S., Squillace, R., Le Menn, G., Rekima, A., Larbret,
- 27 F., Pele, J., Verhasselt, V., Grimaldi, P. A., and Neels, J. G. (2016) A role for Peroxisome Proliferator-
- 28 Activated Receptor Beta in T cell development. *Sci Rep* **6**, 34317
- 29 10. Folch, J., Lees, M., and Sloane Stanley, G. H. (1957) A simple method for the isolation and purification of
- 30 total lipides from animal tissues. *The Journal of biological chemistry* **226**, 497-509
- 31 11. Hur, K. Y., and Lee, M. S. (2015) Gut Microbiota and Metabolic Disorders. *Diabetes Metab J* **39**, 198-203
- 32 12. Kahn, B. B., and Flier, J. S. (2000) Obesity and insulin resistance. *The Journal of clinical investigation* **106**,
- 33 473-481
- 34 13. Le Thuc, O., Stobbe, K., Cansell, C., Nahon, J. L., Blondeau, N., and Rovere, C. (2017) Hypothalamic
- 35 Inflammation and Energy Balance Disruptions: Spotlight on Chemokines. *Front Endocrinol (Lausanne)* **8**,
- 36 197
- 37 14. Montes, V. N., Turner, M. S., Subramanian, S., Ding, Y., Hayden-Ledbetter, M., Slater, S., Goodspeed, L.,
- 38 Wang, S., Omer, M., Den Hartigh, L. J., Averill, M. M., O'Brien, K. D., Ledbetter, J., and Chait, A. (2013)
- 39 T cell activation inhibitors reduce CD8+ T cell and pro-inflammatory macrophage accumulation in adipose
- 40 tissue of obese mice. *PLoS One* **8**, e67709
- 41 15. Yan, L., Song, K., Gao, M., Qu, S., and Liu, D. (2016) Modulation of Cell-Mediated Immunity to Suppress
- 42 High Fat Diet-Induced Obesity and Insulin Resistance. *Pharm Res* **33**, 395-403
- 43 16. Cho, K. W., Morris, D. L., DelProposto, J. L., Geletka, L., Zamarron, B., Martinez-Santibanez, G., Meyer,
- 44 K. A., Singer, K., O'Rourke, R. W., and Lumeng, C. N. (2014) An MHC II-dependent activation loop
- 45 between adipose tissue macrophages and CD4+ T cells controls obesity-induced inflammation. *Cell Rep* **9**,
- 46 605-617
- 47 17. Ibrahim, M. M. (2010) Subcutaneous and visceral adipose tissue: structural and functional differences. *Obes*
- 48 *Rev* **11**, 11-18
- 49 18. Choe, S. S., Huh, J. Y., Hwang, I. J., Kim, J. I., and Kim, J. B. (2016) Adipose Tissue Remodeling: Its Role
- 50 in Energy Metabolism and Metabolic Disorders. *Front Endocrinol (Lausanne)* **7**, 30

- 1 19. Jeffery, E., Wing, A., Holtrup, B., Sebo, Z., Kaplan, J. L., Saavedra-Pena, R., Church, C. D., Colman, L.,
2 Berry, R., and Rodeheffer, M. S. (2016) The Adipose Tissue Microenvironment Regulates Depot-Specific
3 Adipogenesis in Obesity. *Cell metabolism* **24**, 142-150
- 4 20. Liang, X., Kanjanabuch, T., Mao, S. L., Hao, C. M., Tang, Y. W., Declerck, P. J., Hasty, A. H., Wasserman,
5 D. H., Fogo, A. B., and Ma, L. J. (2006) Plasminogen activator inhibitor-1 modulates adipocyte
6 differentiation. *American journal of physiology. Endocrinology and metabolism* **290**, E103-E113
- 7 21. Gustafson, B., and Smith, U. (2006) Cytokines promote Wnt signaling and inflammation and impair the
8 normal differentiation and lipid accumulation in 3T3-L1 preadipocytes. *The Journal of biological chemistry*
9 **281**, 9507-9516
- 10 22. Shin, J. H., Shin, D. W., and Noh, M. (2009) Interleukin-17A inhibits adipocyte differentiation in human
11 mesenchymal stem cells and regulates pro-inflammatory responses in adipocytes. *Biochem Pharmacol* **77**,
12 1835-1844
- 13
- 14
- 15

		FFA (mM)	Cholesterol (mM)
Normal diet	Control	0.77 ± 0.04	1.67 ± 0.07
	Tg T-PPARβ	0.79 ± 0.04	1.87 ± 0.09
High fat diet	Control	0.39 ± 0.05 **	4.13 ± 0.30 ***
	Tg T-PPARβ	0.44 ± 0.05 *	3.76 ± 0.19 **

1 **Table 1: Plasma FFA and cholesterol levels**

2 12 weeks old male mice were exposed to a NC or HFD for 17 weeks. Fasted plasma obtained during GTT was
3 used for free fatty acids (FFA) quantification. Cholesterol levels were measured in unfasted plasma. Data are
4 expressed as mean +/- SEM with n=8 HFD-fed mice and n=7 NC-fed mice. * p<0.05 ; ** p<0.01 ; *** p<0.001
5 between NC and HFD-fed groups.

6

pg/mg protein	High fat diet	
	Control	Tg T-PPAR β
IL-6	107.47 \pm 17.03	80.99 \pm 8.73 *
MCP-1	254.04 \pm 20.55	232.84 \pm 44.12
IL-17a	1725 \pm 96.76	1278 \pm 123 *
PAI-1	2653.75 \pm 227.14	1432.37 \pm 225.78 *
Resistin	7341.25 \pm 929.84	12105 \pm 2288.79
Leptin	20680.51 \pm 1214.56	19707.73 \pm 1540.41

1 **Table 2: EPI-WAT cytokine levels**

2 12 weeks old male mice were exposed to a HFD for 17 weeks. Protein lysate of epididymal adipose tissue was
3 used for cytokine quantification with ELISA (IL-17a) and luminex technology (rest). Data are expressed as
4 mean \pm SEM with n=8 HFD-fed mice. *p<0.05 between control and Tg T-PPAR β mice.

5

1 **FIGURE LEGENDS**

2 **Figure 1: Tg T-PPAR β mice are partially protected against diet-induced obesity**

3 12 weeks old male mice were exposed to a normal diet (NC) or a high-fat diet (HFD) for 17 weeks. (A) Mice
4 body weight at the end of the diet. (B) Mean food intake during the HFD in Kcal/week/g mice. (C) Food
5 efficiency ratio ((mean weight gain (g)/ mean food intake (g))x100) of HFD-fed mice. (D) Total relative activity
6 of HFD-fed mice in metabolic cages. (E) Energy expenditure of HFD-fed mice. (F) mRNA levels of indicated
7 genes relative to 36B4 measured in brown adipose tissue of HFD-fed mice. (G) Quantification of lipid in feces
8 at week 13 of the HFD normalized with feces weight. Data are expressed as mean +/- SEM. n=16 HFD-fed
9 mice and n=7 NC-fed mice, except for (F) where n=4 for control and n=7 for Tg T-PPAR β mice.

10 *p<0.05 ;**p<0.01 between control and Tg T-PPAR β mice.

11
12 **Figure 2: Tg T-PPAR β mice exhibit an amelioration of glucose homeostasis and insulin sensitivity in the**
13 **context of diet-induced obesity**

14 2 weeks old male mice were exposed to a normal diet (NC) or a high-fat diet (HFD) for 17 weeks. (A) Glucose
15 tolerance test (GTT) with weight-matched HFD-fed mice at week 13 of the diet. (B) Insulin tolerance test (ITT)
16 with weight-matched HFD-fed mice at week 11 of the diet. (C) Plasma insulin during GTT expressed in area
17 under curve. (D) Homa-IR index calculated with basal blood glucose and blood insulin during GTT. Data are
18 expressed as mean +/- SEM. n=16 HFD-fed mice and n=7 NC-fed mice. *p<0.05 ;**p<0.01 between control
19 and Tg T-PPAR β mice.

20
21 **Figure 3: HFD-induced liver steatosis is decreased in Tg T-PPAR β mice compared to control mice**

22 12 weeks old male mice were exposed to a HFD for 17 weeks. (A) Liver weight at the end of the HFD. (B)
23 Hepatic triglyceride quantification normalized with liver weight. (C) Liver histology with hematoxylin/eosin
24 staining (10x, scale bar = 200 μ m). (D-G) Expression of indicated genes relative to 36B4 in the liver. Data are
25 expressed as mean +/- SEM. n \geq 10 HFD-fed mice. *p<0.05 ;**p<0.01 ;***p<0.001 between control and Tg T-
26 PPAR β mice.

27
28 **Figure 4: Adipose tissue distribution and function are altered in Tg T-PPAR β mice**

29 12 weeks old male mice were exposed to a HFD for 17 weeks. (A) Sub-cutaneous (WAT-SC) and epididymal
30 (WAT-EPI) adipose tissue weight. (B) Mean adipocyte area in WAT-SC and WAT-EPI calculated from adipose
31 tissue hematoxyline/eosin stainings with Adiposoft software. (C,D) Expression of indicated genes relative to
32 36B4 in the WAT-SC (C) and WAT-EPI (D). Data are expressed as mean +/- SEM. n \geq 10 HFD-fed mice.

33 *p<0.05 ;**p<0.01 ; ***p<0.001 between control and Tg T-PPAR β mice.

1
2
3
4
5
6
7
8
9

Figure 5: Decreased adipose tissue inflammation and $\alpha\beta/\gamma\delta$ T cell ratio in HFD-fed Tg T-PPAR β mice

Flow cytometric analysis on stromal vascular fraction of epididymal adipose tissue of HFD-fed mice. (A,B) Total (F4/80+CD11b+), proinflammatory (F4/80+ CD11b+ CD11c+) and anti-inflammatory macrophages (F4/80+ CD11b+ CD11c-) in proportion (A) and cell number (B). (C) Ratio of CD11c+/CD11c- macrophages in epididymal adipose tissue. (D,E) T cell populations based on CD3, CD4, CD8, TCR β and TCR $\gamma\delta$ expression in proportion (D) and cell number (E). (F) $\alpha\beta/\gamma\delta$ T cell ratio in epididymal adipose tissue. Data are expressed as mean +/- SEM. n \geq 10 HFD fed mice. *p<0.05 ;**p<0.01 between control and Tg T-PPAR β mice.

Figure 1

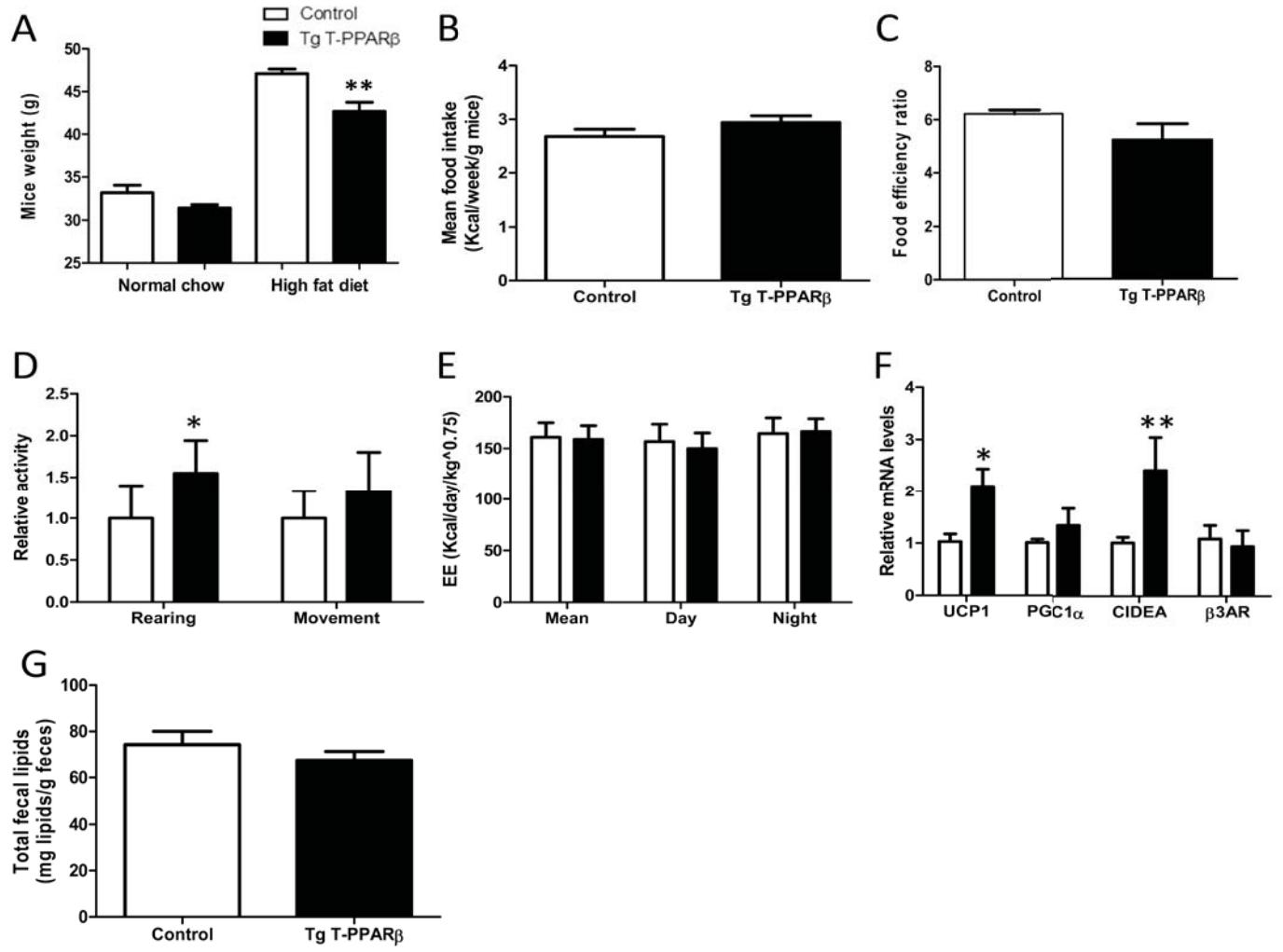


Figure 2

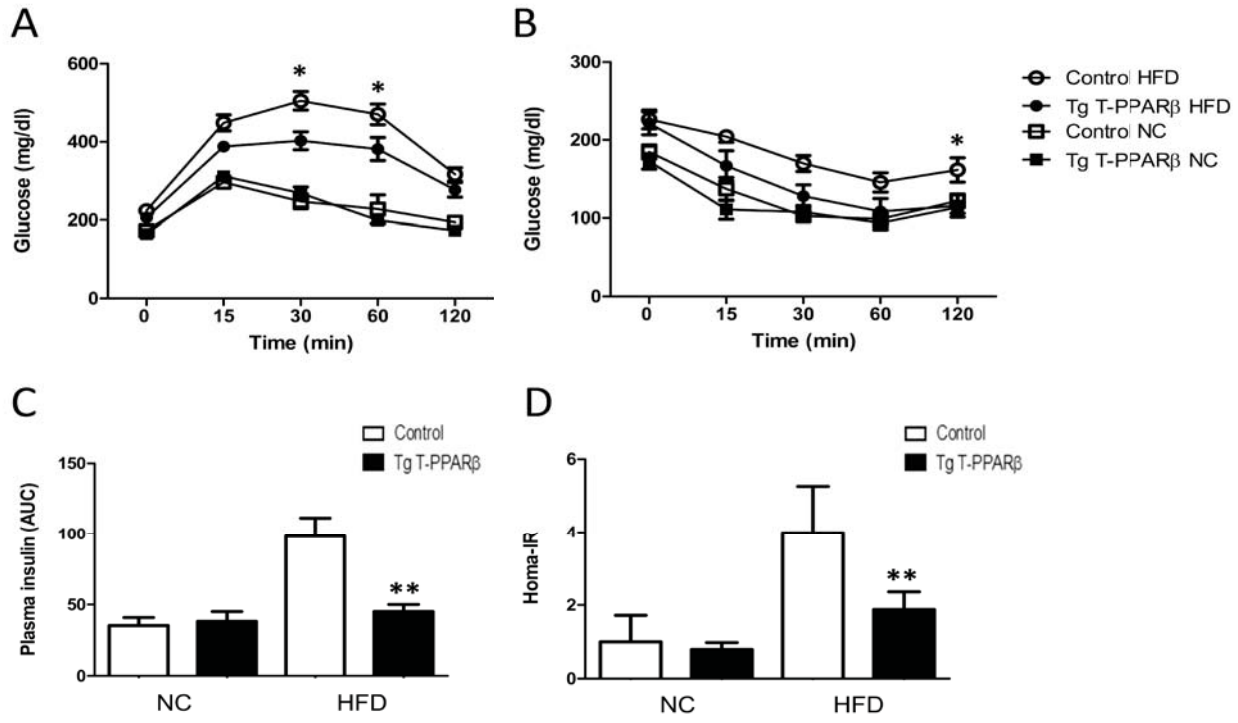


Figure 3

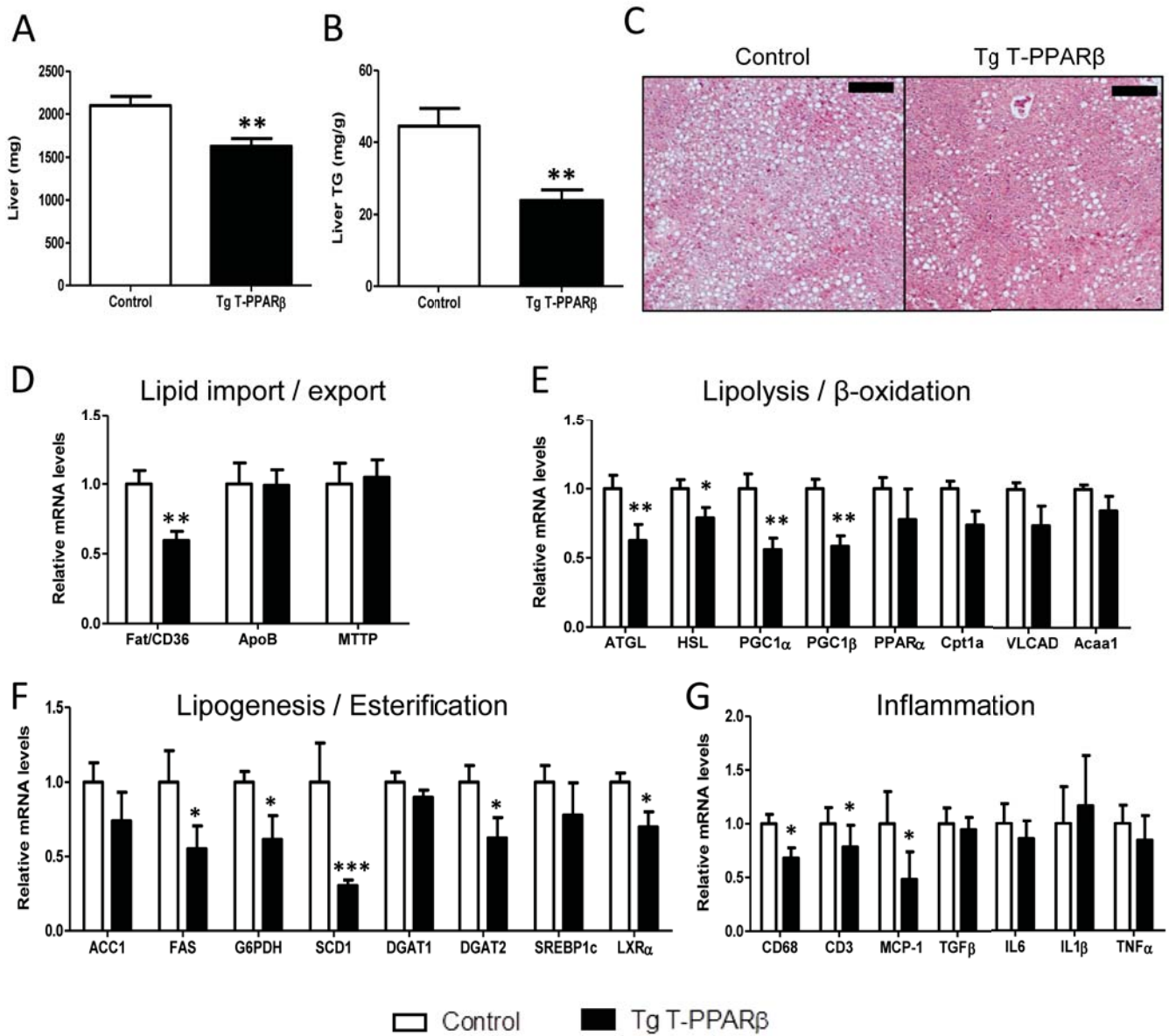


Figure 4

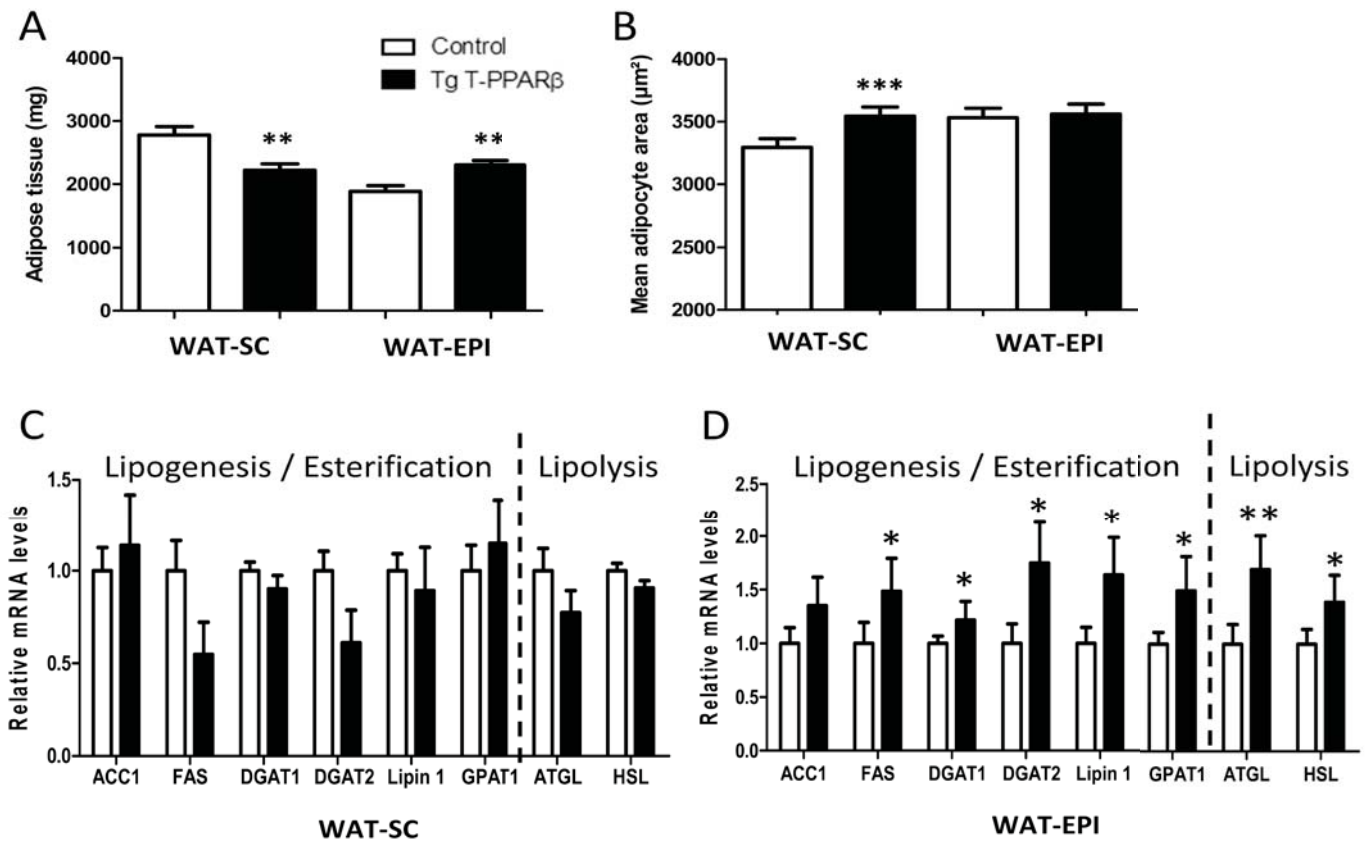
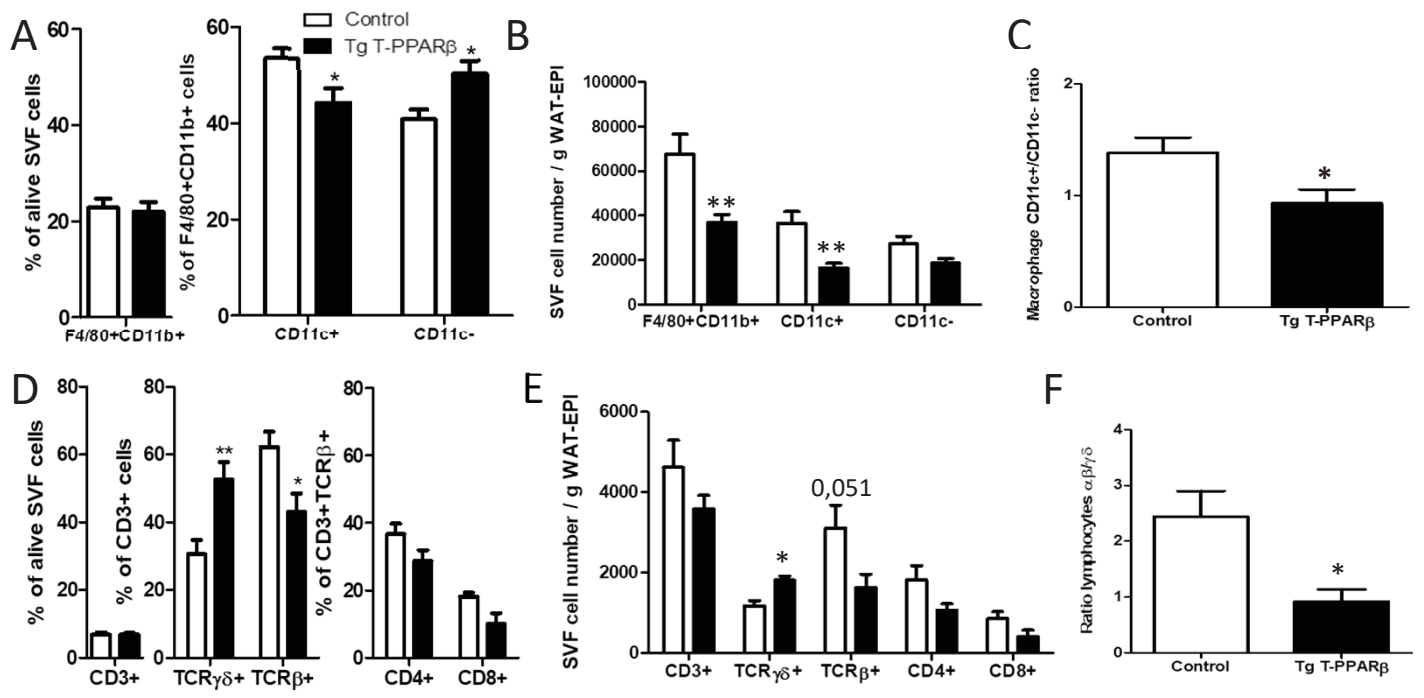


Figure 5



Supplemental Data

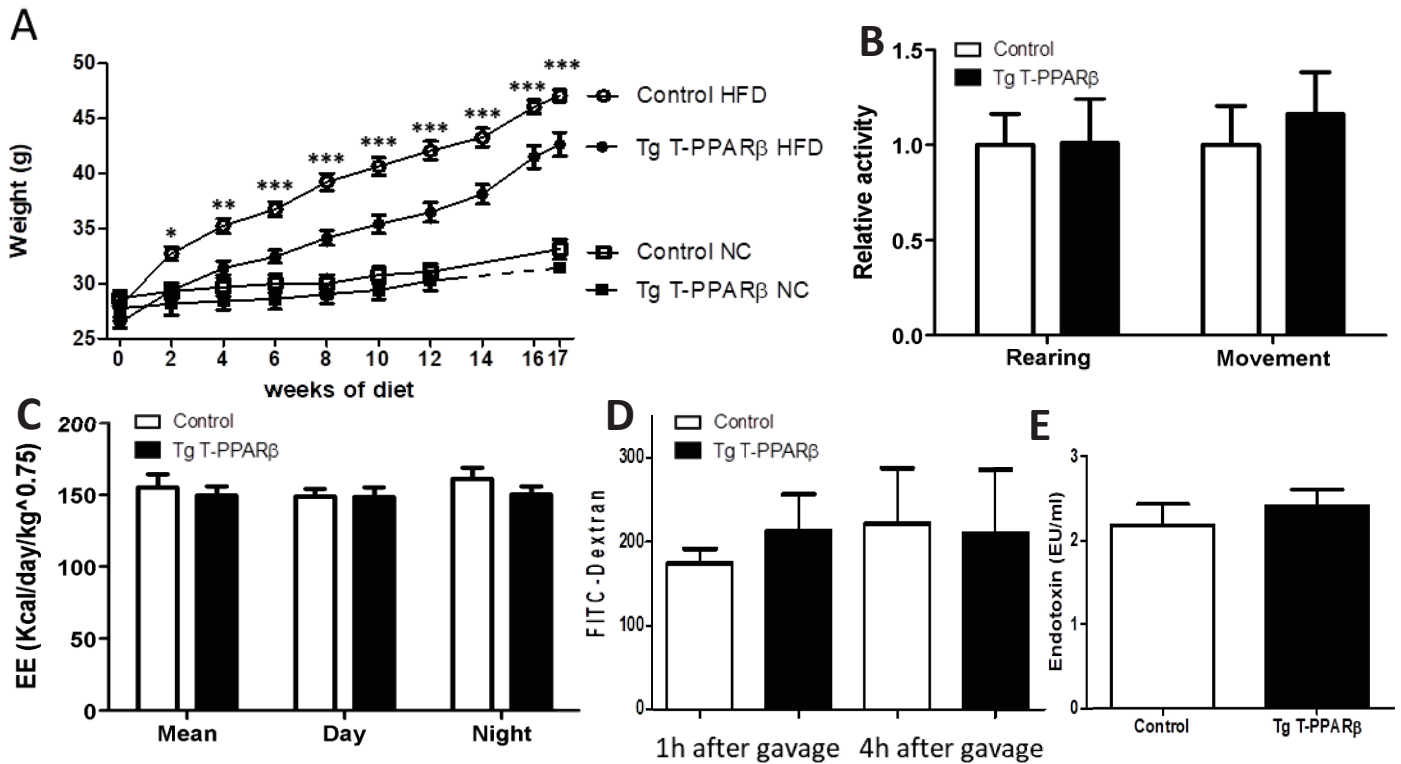


Figure S1: Weight gain, relative activity, energy expenditure and intestinal permeability in Tg T-PPAR β compared to control mice. 12 weeks old male mice were exposed to a normal diet (NC) or a high-fat diet (HFD) for 17 weeks. (A) Mice body weight during the diet. (B) Total relative activity of NC-fed mice in metabolic cages. (C) Energy expenditure of NC-fed mice. (D) Quantification of blood FITC at one or four hours after a FITC-dextran gavage in HFD-fed groups. (E) Quantification of plasmatic endotoxin levels in HFD-fed groups. Data are expressed as mean \pm SEM. $n=16$ HFD-fed mice and $n=7$ NC-fed mice. * $p<0.05$; ** $p<0.01$; *** $p<0.001$ between control and Tg T-PPAR β mice.

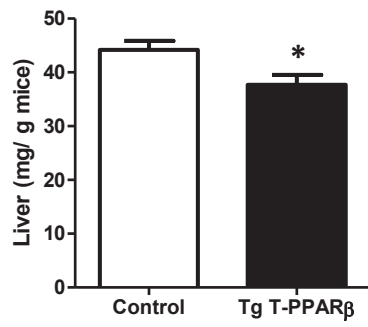


Figure S2: Liver weight normalized to mice body weight at the end of the high fat diet. Data are expressed as mean \pm SEM. $n \geq 10$ HFD-fed mice. * $p < 0.05$ between control and Tg T-PPAR β mice.

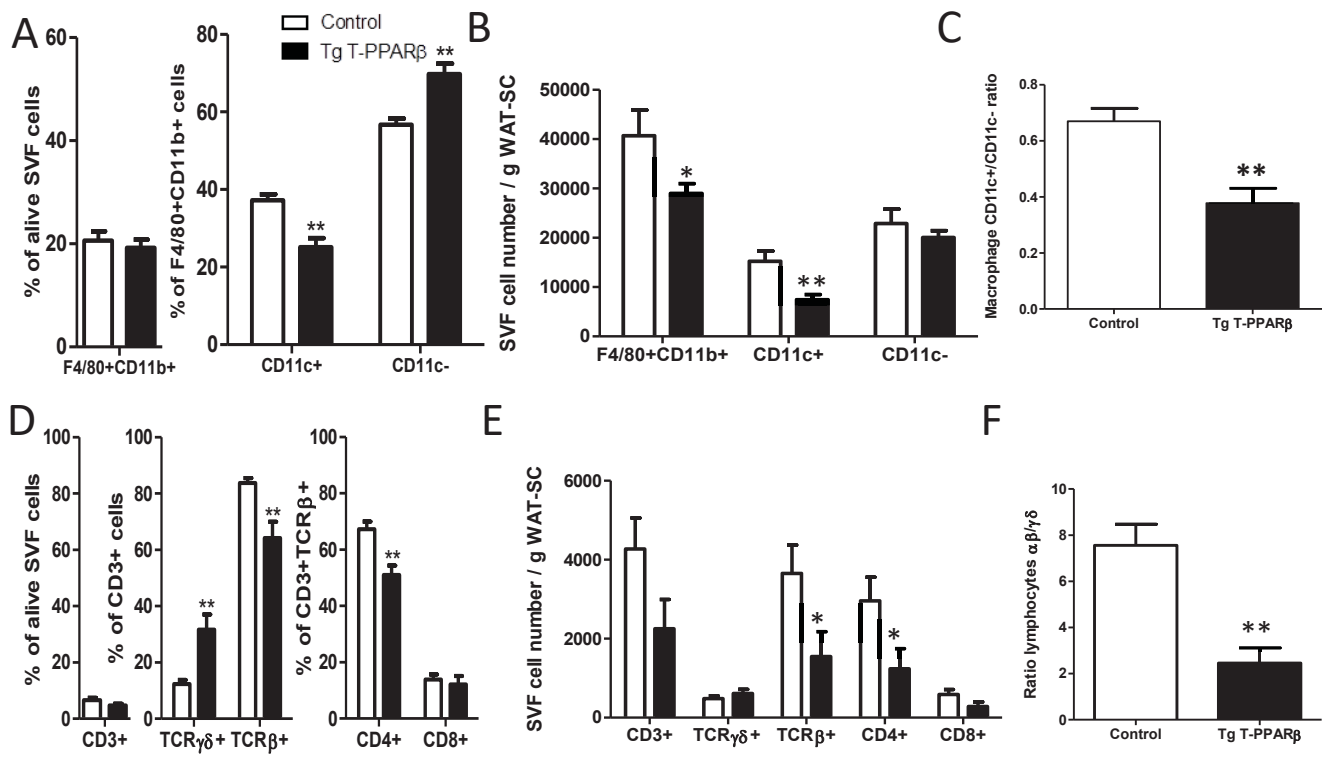


Figure S3: Flow cytometric analysis on stromal vascular fraction of sub-cutaneous adipose tissue of HFD-fed mice. (A,B) Total (F4/80+CD11b+), proinflammatory (F4/80+ CD11b+ CD11c+) and anti-inflammatory macrophages (F4/80+ CD11b+ CD11c-) in proportion (A) and cell number (B). (C) Ratio of CD11c+/CD11c- macrophages in sub-cutaneous adipose tissue. (D,E) T cell populations based on CD3, CD4, CD8, TCRβ and TCRγδ expression in proportion (D) and cell number (E). (F) αβ/γδ T cell ratio in sub-cutaneous adipose tissue. Data are expressed as mean +/- SEM. n≥10 HFD fed mice. *p<0.05 ; **p<0.01 between control and Tg T-PPARβ mice.